# Cavity cooling of an optically levitated submicron particle

Nikolai Kiesel[1,2], Florian Blaser[1], Uroš Delić, David Grass, Rainer Kaltenbaek, and Markus Aspelmeyer[2]

Vienna Center for Quantum Science and Technology (VCQ), Faculty of Physics, University of Vienna, A-1090 Vienna, Austria

Edited by David A. Weitz, Harvard University, Cambridge, MA, and approved July 16, 2013 (received for review May 14, 2013)

**The coupling of a levitated submicron particle and an optical cavity field promises access to a unique parameter regime both for macroscopic quantum experiments and for high-precision force sensing. We report a demonstration of such controlled interactions by cavity cooling the center-of-mass motion of an optically trapped submicron particle. This paves the way for a light–matter interface that can enable room-temperature quantum experiments with mesoscopic mechanical systems.**

optical trapping | quantum optics | cavity optomechanics | nanoparticles | nanomechanics

The ability to trap and to manipulate individual atoms is at the heart of current implementations of quantum simulations (1, 2), quantum computing (3), and long-distance quantum communication (4, 5). Controlling the motion of larger particles opens up avenues for quantum science, both for the study of fundamental quantum phenomena in the context of matter wave interference (6), and for unique sensing and transduction applications in the context of quantum optomechanics (7, 8). Specifically, it has been suggested that cavity cooling of a single submicron particle in high vacuum allows for the generation of quantum states of motion in a room-temperature environment (9–11), as well as for unprecedented force sensitivity (12, 13). Here, we take steps into this regime. We demonstrate cavity cooling of an optically levitated submicron particle consisting of $\sim 10^9$ atoms (estimated diameter of 340 nm). The particle is trapped at modest vacuum levels of a few millibars in the standing-wave field of an optical cavity and is cooled through coherent scattering into the modes of the same cavity (14, 15). We estimate that our cooling rates are sufficient for ground-state cooling, provided that optical trapping at a vacuum level of $10^{-7}$ mbar can be realized in the future, e.g., by using additional active-feedback schemes to stabilize the optical trap in three dimensions (16–19).

Cooling and coherent control of single atoms inside an optical cavity are well-established techniques within atomic quantum optics (20–24). The main idea of cavity cooling relies on the fact that the presence of an optical cavity can resonantly enhance scattering processes of laser light that deplete the kinetic energy of the atom, specifically those processes where a photon that is scattered from the atom is Doppler shifted to a higher frequency. It was realized early on that such cavity-enhanced scattering processes can be used to achieve laser cooling even of objects without exploitable internal level structure such as molecules and submicron particles (14, 15, 25, 26). For nanoscale objects, cavity cooling has been demonstrated in a series of recent experiments with nanobeams (27–29) and membranes of nanometer-scale thickness (e.g., refs. 30 and 31). To guarantee long interaction times with the cavity field, these objects were mechanically clamped, which however introduces additional dissipation and heating through the mechanical support structure. As a consequence, quantum signatures have thus far only been observed in a cryogenic environment (32, 33). Freely suspended particles can circumvent this limitation and allow for far better decoupling of the mesoscopic object from the environment. This has been successfully implemented for atoms driven at optical frequencies far detuned from the atomic resonances, both for the case of optically trapped single atoms (22, 23) and for clouds of up to $10^5$ ultracold atoms (34–36). In comparison to such clouds, massive solid objects provide access to a different parameter regime: on the one hand, the rigidity of the object allows to manipulate the center-of-mass (CM) motion of the whole system, thus enabling macroscopically distinct superposition states (10, 11, 37); on the other hand, the large mass density of solids concentrates many atoms in a small volume of space, which provides unique perspectives for force sensing (12, 13). In our work, we have now extended the scheme to dielectric submicron particles comprising up to $10^9$ atoms. By using a high-finesse optical cavity for both optical trapping and manipulation, we demonstrate cavity-optomechanical control, including cooling, of the CM motion of a levitated solid object without internal level structure.

To understand the principle of our approach, consider a dielectric spherical particle of radius $r$ smaller than the optical wavelength $\lambda$. Its finite polarizability $\xi = 4\pi\epsilon_0 r^3 Re\left\{\frac{\epsilon-1}{\epsilon+2}\right\}$ ($\varepsilon$: dielectric constant; $\epsilon_0$: vacuum permitivity) results in an optical gradient force that allows to trap particles in the intensity maximum of an optical field (38). The spatial modes of an optical cavity provide a standing-wave intensity distribution along the cavity axis $x$. A submicron particle that enters the cavity will be pulled toward one of the intensity maxima, located a distance $x_0$ from the cavity center. For the case of a Gaussian (TEM00) cavity mode, the spatial profile will result in radial trapping around the cavity axis, hence providing a full 3D particle confinement. In addition, Rayleigh scattering off the particle into the cavity mode induces a dispersive change in optical path length and shifts the cavity resonance frequency by $U_0(x_0) = \frac{\omega_{cav}\xi}{2\epsilon_0 V_{cav}}\left(1 + \frac{x_0^2}{x_R^2}\right)$ (39) ($\omega_{cav}$: cavity frequency; $V_{cav}$: cavity mode volume; $x_R$: cavity-mode Rayleigh length). This provides the underlying optomechanical coupling mechanism between the CM motion of a particle moving along the cavity axis and the photons of a Gaussian cavity mode. The resulting interaction Hamiltonian is as follows (e.g., ref. 40):

$$H_{int} = -\hbar U_0(x_0)\hat{n}\sin^2\left(kx_0 + k\bar{x} + k\hat{x}\right),$$

where we have allowed for a mean displacement $\bar{x}$ of the submicron particle with respect to the intensity maximum $x_0$ ($\hat{x}$: CM position operator of the trapped submicron particle; $k = \frac{2\pi}{\lambda}$: wave number of the cavity light field; $\hat{n}$: cavity photon number operator).

Author contributions: N.K., F.B., and M.A. designed research; N.K., F.B., U.D., D.G., R.K., and M.A. performed research; N.K., F.B., U.D., D.G., R.K., and M.A. analyzed data; and N.K., F.B., U.D., D.G., R.K., and M.A. wrote the paper.

The authors declare no conflict of interest.

This article is a PNAS Direct Submission.

Freely available online through the PNAS open access option.

[1]N.K. and F.B. contributed equally to this work.

[2]To whom correspondence may be addressed. E-mail: nikolai.kiesel@univie.ac.at or markus.aspelmeyer@univie.ac.at.

This article contains supporting information online at www.pnas.org/lookup/suppl/doi:10.1073/pnas.1309167110/-/DCSupplemental.

For the case of a single optical cavity mode, the particle is trapped at an intensity maximum ($\bar{x}=0$), and, for small displacements, only coupling terms that are quadratic in $\hat{x}$ are relevant (30). Linear coupling provides intrinsically larger coupling rates and can be exploited for various quantum control protocols (41). However, it requires to position the particle outside the intensity maximum of the field. This can be achieved for example by an optical tweezer external to the cavity (10), by harnessing gravity in a vertically mounted cavity (42) or by using a second cavity mode with longitudinally shifted intensity maxima (9, 10).

We follow the latter approach and operate the optical cavity with two longitudinal Gaussian modes of different frequency, namely, a strong "trapping field" to realize a well-localized optical trap at one of its intensity maxima, and a weaker "control field" that couples to the particle at a shifted position $\bar{x}\neq 0$. For localization in the Lamb–Dicke regime ($k^2\langle\hat{x}^2\rangle \ll 1$) this yields (8, 43) linear optomechanical coupling between the trapped particle and the control field at a rate $g_0 = U_0(x_0)\sin(2k\bar{x})k\sqrt{\frac{\hbar}{m\Omega_0}}$ per photon ($m$: particle mass; $\Omega_0$: frequency of CM motion). Detuning of the control field from the cavity resonance by a frequency $\Delta=\omega_{cav}-\omega_c$($\omega_c$ : control field frequency) results in the well-known dynamics of cavity optomechanics (8). Specifically, the position dependence of the gradient force will change the stiffness of the optical trap, shifting $\Omega_0$ to an effective frequency $\Omega_{\text{eff}}$ (optical spring), and the cavity-induced retardation of the force will introduce additional optomechanical (positive or negative) damping on the particle motion. From a quantum-optics viewpoint, the oscillating submicron particle scatters photons into optical sidebands of frequencies $\omega_c\pm\Omega_0$ at rates $A_\pm=\frac{1}{4}\frac{g_0^2\langle\hat{n}\rangle\kappa}{(\kappa/2)^2+(\Delta\pm\Omega_0)^2}$, known as Stokes and anti-Stokes scattering, respectively ($\kappa$: FWHM cavity line width). For $\Delta>0$ (red detuning), anti-Stokes scattering becomes resonantly enhanced by the cavity, effectively depleting the kinetic energy of the submicron particle motion via a net laser-cooling rate of $\Gamma=A_- - A_+$. In the following, we demonstrate all these effects experimentally with an optically trapped silica submicron particle.

As is shown in Fig. 1, our setup comprises a high-finesse Fabry–Perot cavity (Finesse $F=76000$; $\kappa=2\pi\times 180$kHz) that is mounted inside a vacuum chamber kept at a pressure between 1 and 5 mbar. Airborne silica submicron particles (specified with radius $r=127\pm 13$nm) are emitted from an isopropanol solution via an ultrasonic nebulizer and are trapped inside the cavity in the standing wave of the trapping field (*Materials and Methods*). To achieve the desired displacement between the intensity maxima of trapping field and control field ($\bar{x}\neq 0$), we use the adjacent longitudinal cavity mode for the control beam, i.e., the cavity mode shifted by approximately one free spectral range $\text{FSR}=\frac{c}{2L}\approx 13.67$ GHz in frequency from the trapping beam ($c$: vacuum speed of light; $L$: cavity length). Depending on the distance from the cavity center $x_0$, the two standing-wave intensity distributions are then shifted with respect to each other by $\frac{\lambda}{2L}(x_0+L/2)$ (Fig. 1*B*). For example, to achieve maximal coupling $g_0$ for weak control beam powers, i.e., for $\mu=\frac{P_c}{P_t}\ll 1$ [$P_{c(t)}$: power of control (trapping) beam in the cavity], the submicron particle needs to be positioned at $x_0=L/4$, where the antinodes of the two beams are separated by $\lambda/8$ (9, 10). Note that when the control beam is strong enough to significantly contribute to the optical trap ($\mu\gtrapprox 0.1$), the displacement $\bar{x}$ and both $\Omega_0$ and $g_0$ are modified when $\mu$ is changed (35). The exact dependence of these optomechanical parameters on $\mu$ depends on $x_0$ (*SI Text*, section 1).

The optomechanical coupling between the control field and the particle can be used to both manipulate and detect the

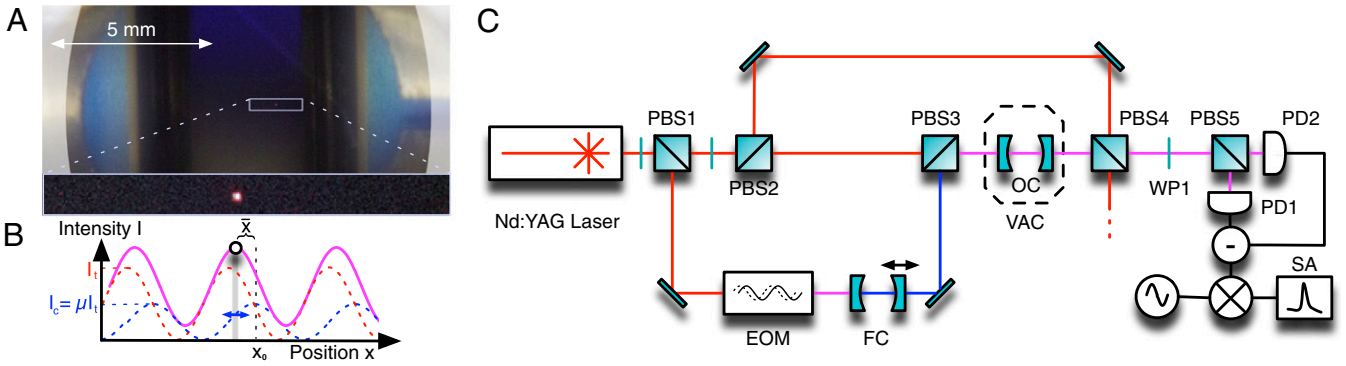


**Fig. 1.** Optical trapping and readout of a submicron particle in a Fabry–Perot cavity. (*A*) Submicron particle in a cavity. A photo of our near-confocal Fabry–Perot optical cavity (OC) [F = 76,000; $L=\frac{c}{2\text{FSR}}=10.97$mm, determined via the free spectral range (FSR)]. The white-shaded areas indicate the curvature of the cavity mirrors. The optical field between the mirrors traps a submicron particle. The enlarged *Inset* shows light scattered by the submicron particle. (*B*) Schematics of two-mode optical trap and dispersive coupling. Two optical fields form standing-wave intensity distributions along the optical cavity axis (dashed lines; blue: control beam; red: trapping beam). Because of their different frequencies, the intensity maxima of the two fields are displaced with respect to each other. A submicron particle is trapped at the maximum of the total intensity distribution (purple solid line). Because the trapping beam is more intense than the control beam, the submicron particle is trapped at a distance $\bar{x}\neq 0$ away from the control beam intensity maximum $x_0$. As a consequence, the submicron particle oscillates within a region where the control beam intensity varies with the particle position (blue arrow), resulting in linear dispersive coupling (see main text and *SI Text*, section 1). The displacement $\bar{x}$ depends on the ratio between the intensity maxima of the two fields. (*C*) Experimental setup. A Nd:YAG laser ($\lambda=1,064$ nm) is split into three beams at the polarizing beam splitters PBS1 and PBS2. Wave plates (shown as green lines in the figure) are used to set the power of the beams. The transmitted beam is used to lock the laser to the TEM00 mode of the OC and provides the trapping field for the submicron particle. The beam reflected at PBS1 is used to prepare the control beam, which is frequency shifted by $\delta\omega$ close to the adjacent cavity resonance of the TEM00 mode, i.e., $\delta\omega=\text{FSR}+\Delta$ ($\Delta$: detuning from cavity resonance). The single-frequency side band at $\delta\omega$ is created using an electrooptical modulator (EOM) followed by optical amplification in fiber and transmission through a filtering cavity (FC) with an FWHM line width of $2\pi\times 500$ MHz. The control and trapping beams are overlapped at PBS3 and transmitted through the OC with orthogonal polarizations. The OC is mounted inside a vacuum chamber (VAC). When a submicron particle is trapped in the optical field in the cavity, its center-of-mass (CM) motion introduces a phase modulation on the control beam. To detect this signal, we perform interferometric phase readout of the control beam: At PBS4, the control beam is separated from the trapping beam and spatially overlapped with the local oscillator (LO). Note that the LO and the control beam are orthogonally polarized. After a polarization rotation by 45° at WP1, PBS5 serves to superimpose the control beam with the LO resulting in interference in its two output ports, where high-frequency InGaAs photo detectors PD1 and PD2 detect the resulting beat signal. We mix (multiply) the difference signal of the two detectors with an ELO of frequency $\text{FSR}+\Delta$ and record the NPS of the resulting signal using a spectrum analyzer (SA) (see *Materials and Methods* and *SI Text*, section 2, for more detail).

particle motion. Specifically, the axial motion of the submicron particle generates a phase modulation of the control field, which we detect by heterodyne detection (*Materials and Methods*). We reconstruct the noise power spectrum (NPS) of the mechanical motion by taking into account the significant filtering effects exhibited by the cavity (arising from the fact that $\kappa \approx \Omega_0$) on the transmitted control beam (*SI Text*, section 2). Assuming a particle size of 170-nm radius, as inferred from the particle polarizability (see below), we estimate the position sensitivity of our readout scheme to be $4\text{pm}/\sqrt{\text{Hz}}$. It is likely limited by classical laser noise (see below).

The properties of our optical trap are summarized in Fig. 2. The influence of the control beam on the trapping potential is purposely kept small by choosing $\mu \approx 0.1$ and $\Delta \approx 0$. We expect that the axial mechanical frequency $\Omega_0$ depends both on the power of the trapping beam $P_t$ and on $x_0$ through the cavity beam waist $W(x_0)$ via $\Omega_0 = \sqrt{\frac{12k^2}{c\pi} Re\left(\frac{1}{\rho}\frac{\epsilon-1}{\epsilon+2}\right)} \cdot \sqrt{\frac{P_t}{\pi W(x_0)}}$ (9, 10), in agreement with our data. The damping $\gamma_0$ of the mechanical resonator is dominated by the ambient pressure of the background gas down to a few millibars (Fig. 2*B*). Below these pressures, the submicron particle is not stably trapped anymore, whereas trapping times up to several hours can be achieved at a pressure of a few millibars. This is a known, yet unexplained phenomenon (17, 18, 44). Reproducible optical trapping at lower pressure values has thus far only been reported using feedback cooling in three dimensions for the case of microparticles and nanoparticles (17, 18) or, without feedback cooling, with particles of at least 20-μm radius (45).

We finally demonstrate cavity-optomechanical control of our levitated submicron particle. All measurements have been performed with the same particle for an intracavity trapping beam power $P_t$ of ∼55 W and at a pressure of $p \approx 4$ mbar. This corresponds to a bare mechanical frequency $\Omega_0/2\pi = 165 \pm 3$kHz and an intrinsic mechanical damping rate $\gamma_0/2\pi = 7.2 \pm 0.8$kHz, respectively. Fig. 3*A* shows the dependence of a typical NPS of the particle's motion upon detuning of the control field. Note that the power ratio $\mu$ between trapping beam and control beam is kept constant, which is achieved by adjusting the control beam power for different detunings. The amplitude scale, as well as the temperature scale in Fig. 3*E*, is calibrated through the NPS measurement performed close to zero detuning ($\Delta = 1$kHz; blue NPS in Fig. 3*A*) by using the equipartition theorem for $T = 293$ K. This is justified by an independent measurement that verifies thermalization of the CM mode at zero detuning for our parameter regime (*SI Text*, section 4). Both the inferred effective mechanical frequency $\Omega_{\text{eff}}$ (Fig. 3*B*) and the effective mechanical damping $\gamma_{\text{eff}}$ (Fig. 3*C*) show a systematic dependence on the detuning $\Delta$ of the control beam, in good agreement with the expected dynamical backaction effects for linear optomechanical coupling (*SI Text*, section 1). A fit of the expected theory curve to the optical spring data allows estimating the strength of the optomechanical coupling for different values of $\mu$ (Fig. 3*D*). If the position $x_0$ of the submicron particle in the cavity is known, then this behavior is uniquely determined by $U_0(x_0)$. For a particle position $x_0 = 1.56 \pm 0.14$mm, which was determined independently with a CCD camera, we find $U_0(x_0) = 2\pi \times (145 \pm 2)$kHz. These values allow to infer a submicron particle displacement

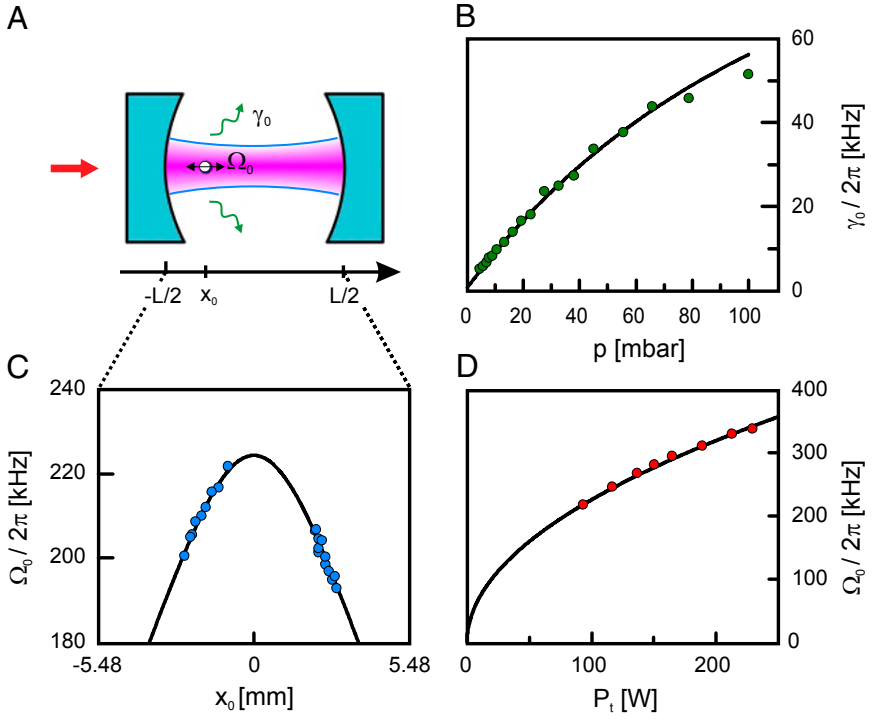


**Fig. 2.** Experimental characterization of the submicron particle cavity trap. (*A*) Schematic of the trap configuration. An optical cavity of length $L = 10.97$ mm is driven on resonance of a Gaussian TEM00 cavity mode by a laser with a wavelength of $\lambda = 1,064$ nm. The submicron particle is optically trapped at position $x_0$. Its CM motion in the axial direction of the cavity is described by a harmonic oscillator with a frequency $\Omega_0$ and an amplitude of ∼10 nm . In addition, the submicron particle experiences collisions with the surrounding gas resulting in a damping rate $\gamma_0$. (*B*) Mechanical damping $\gamma_0$ as a function of pressure. The solid line is a fit of kinetic gas theory to the data (*SI Text*, section 4). (*C*) Position-dependent trapping frequency. The waist of the optical mode expands from ∼41 μm at the cavity center to 61 μm at the cavity mirrors, resulting in a position-dependent trapping potential. Here, we show the corresponding change of the trapping frequency $\Omega_0$ with the position of the submicron particle. (*D*) Power-dependent trapping frequency. We experimentally show the dependence of the trapping frequency on the intracavity power $P_t$. The solid lines in *C* and *D* are based on the theoretical model as described in the main text, with a scaling factor as the only free fit parameter.

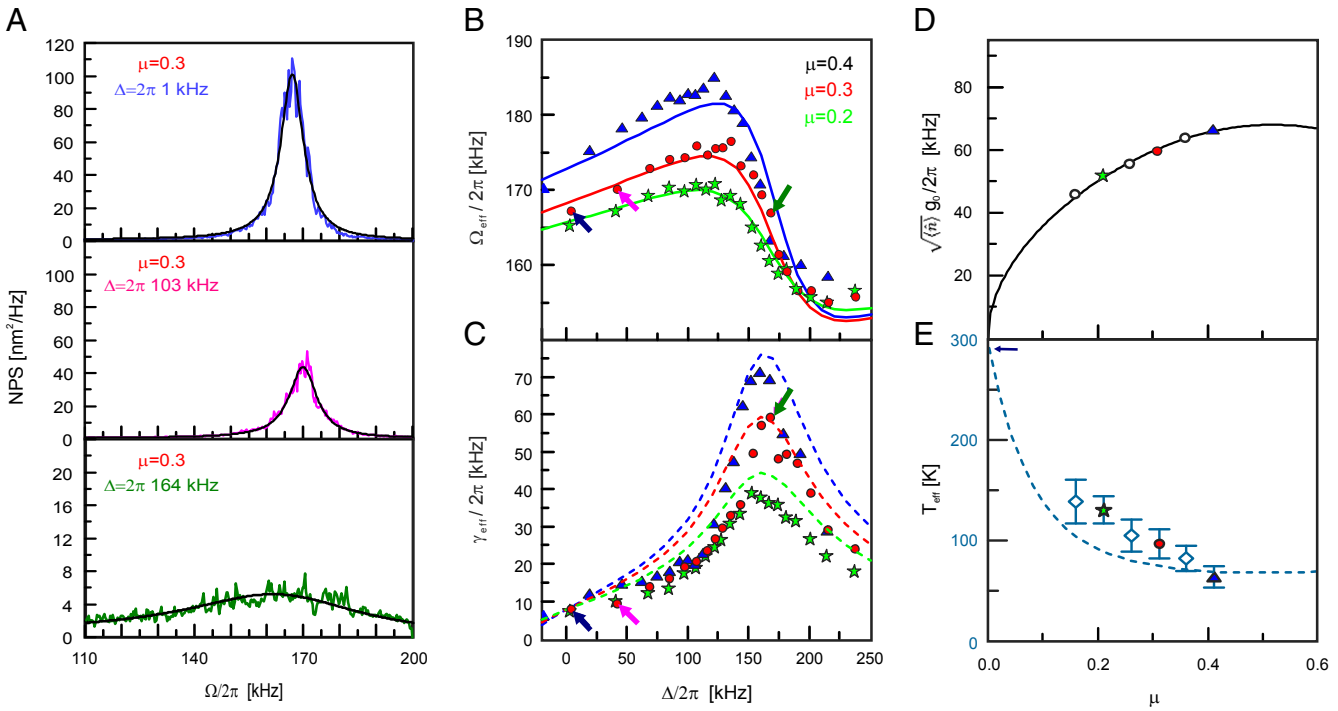


**Fig. 3.** Cavity-optomechanical control and cooling of a submicron particle. We obtain noise power spectra (NPS) (*A*) of the submicron particle's CM motion for different settings of the control-beam power $P_c$ and detuning $\Delta$. During each measurement, $\mu = \frac{P_c}{P_t}$ was kept constant ($P_t$: trapping beam power). Based on these NPS, we determine the effective mechanical frequency $\Omega_{\text{eff}}$ and line width $\gamma_{\text{eff}}$ of the optomechanical system, and its effective temperature $T_{\text{eff}}$. We study the modification of these spectra caused by optomechanical interaction in *B*, *C*, and *E*. Based on the data in *B*, we infer the power-dependent strength of optomechanical coupling in *D*. (*A*) Mechanical noise power spectra. Shown are examples of the mechanical NPS measured for constant control-beam power ($\mu = 0.3$) at three different detunings $\Delta$ with respect to the cavity resonance frequency. The detuning results in a significant modification of the NPS due to optomechanical effects. Note that scale is changed by a factor of 5 in the bottom plot in *A*. To determine the effective mechanical frequency $\Omega_{\text{eff}}$ and line width $\gamma_{\text{eff}}$ of the optomechanical system, we fit the NPS of an harmonic oscillator (black solid lines) to this data. We infer the value of the effective temperature $T_{\text{eff}}$ from the equipartition theorem via direct integration of the NPS (*SI Text*, section 3). (*B*) Optical spring. When the control beam is red-detuned from the cavity resonance ($\Delta > 0$), we observe a characteristic modification of the mechanical frequency $\Omega_{\text{eff}}$. The solid lines in *B* correspond to a theoretical model that is fitted to the data for each value of $\mu$. The optomechanical coupling $g_0\sqrt{\langle \hat{n} \rangle}$ is one of the fit parameters (*SI Text*, section 3). Based on these results for the optical spring, we calculate the theoretical expectations for $\gamma_{\text{eff}}$ and $T_{\text{eff}}$, which are shown as dashed lines in *C* and *E*. (*C*) Optomechanical damping. Line width broadening of the mechanical resonance as a function of the detuning $\Delta$. (*D*) Optomechanical coupling. We infer the optomechanical coupling rate $g_0\sqrt{\langle \hat{n} \rangle}$ from the strength of the optical spring (*B*) and show its dependence on the power ratio $\mu$. This relation depends on the position $x_0$ of the submicron particle in the cavity. For the data presented here, we determine $x_0 = 1.56 \pm 0.14$ mm (*SI Text*, section 5). We find very good agreement between the data and the theoretical model, where only the submicron particle polarizability serves as a fit parameter (solid line; *SI Text*, section 3). (*E*) Cavity cooling. The decrease in effective temperature $T_{\text{eff}}$ is shown for increasing control beam power. To obtain a good estimate of the measurement error, we average over measurements taken for detunings between $\Delta$ = 100–150 kHz (*SI Text*, section 3). The dashed line is a theoretical prediction based on the parameters obtained from the fit to the optical spring data (*B*).

$\bar{x} \approx 0.15 \times (\lambda/2) = 77$nm, yielding a fundamental single-photon coupling rate $g_0 \approx 2\pi \times 1.2$Hz (for $\mu \to 0$). Assuming a (supplier-specified) material density of $\rho = 1,950 \text{g/cm}^3$and a dielectric constant $\epsilon_{\text{SiO}_2} = 2.1$, our results indicate a single trapped submicron particle of radius $r \approx 169$nm.

The red-detuned driving of the cavity by the control laser also cools the CM motion of the levitated submicron particle through coherent scattering into the cavity modes. Fig. 3*E* shows the resulting effective temperature as deduced from the area of the NPS of the mechanical motion by applying the equipartition theorem. The experimental data are well in agreement with the expected theory for cavity cooling (*SI Text*, section 1). We achieve cooling rates of up to $\Gamma = 2\pi \times 49$ kHz and effective optomechanical coupling rates of up to $g_0\sqrt{\langle \hat{n}_c \rangle} = 2\pi \times 66$ kHz ($\langle \hat{n}_c \rangle$: mean photon number in control field), comparable to state-of-the-art clamped mechanical systems in that frequency range (8). The demonstrated cooling performance, with a minimal CM-mode temperature of $64 \pm 5$K, is only limited by damping through residual gas pressure that results in a mechanical quality of $Q = \frac{\Omega_0}{\gamma_0} \approx 25$. Recent experiments (17, 18) impressively demonstrate that lower pressures can be achieved when cooling is applied in all three spatial dimensions. Cooling the transverse motion of the particle will also avoid unwanted heating in the axial direction due to the anharmonicity of the optical trap (*SI Text*, section 6). Given the fact that our cavity-induced longitudinal cooling rate is comparable to the feedback cooling rates achieved in those experiments, a combined scheme should eventually be capable of performing quantum experiments at moderately high vacuum levels. For example, our cooling rate is in principle sufficient to obtain cooling to the quantum ground state of the CM motion starting from room temperature with a longitudinal mechanical quality factor of $Q \approx 10^9$, i.e., a vacuum level of $10^{-7}$ mbar. Such a performance is currently out of reach for other existing cavity optomechanical systems with comparable frequencies. In addition, even larger cooling rates are expected when both beams are red-detuned to cooperatively cool the submicron particle motion (44).

Our experiment constitutes a first proof of concept demonstration in that direction. We envision that, once this level of performance is achieved, levitated submicron particles in optical cavities will provide a room-temperature quantum interface between light and matter, along the lines proposed in refs. 9, 10,

PHYSICS

and 41, with new opportunities for macroscopic quantum experiments in a regime of large mass (11, 37, 46). The large degree of optomechanical control over levitated objects may also enable applications in other areas of physics such as for precision force sensing (12, 13) or for studying nonequilibrium dynamics in classical and quantum many-body systems (47).

## Materials and Methods

**Loading of Submicron Particles into the Optical Cavity Trap.** For our experiment, we use silica nanospheres (Corpuscular) with a specified radius of $r = 127 \pm 13$nm, which are provided in an aqueous solution with a mass concentration of 10%. We dilute the solution with isopropanol to a mass concentration of $10^{-7}$ and keep it for ∼30 min in an ultrasonic bath before use. To obtain airborne submicron particles, an ultrasonic medical nebulizer (Omron Micro Air) emits droplets from the solution with ∼3-μm size (44, 48). On average, the number of nanospheres per droplet is then $\sim 5 \cdot 10^{-4}$.

The nanospheres are loaded into the vacuum chamber by spraying the droplets through an inlet valve at the end of a 6-mm–thick, 90-cm–long steel tube. We keep the pressure inside the vacuum chamber between 1 and 5 mbar via manual control of both the inlet valve connected to the nebulizer and the outlet valve connected to the vacuum pumps. During the loading process, the trapping laser is kept resonant with the cavity at the desired intracavity power for optical trapping. The low pressure minimizes pressure-induced fluctuations of the optical path length, which significantly simplifies locking the laser to the cavity.

Trapping in the conservative potential of the standing-wave trap is only possible with an additional dissipative process, which is provided fully by damping due to the remaining background gas. Within a few seconds after opening the valve, nanospheres get optically trapped. The standing-wave configuration provides multiple trapping positions. Trapped submicron particles are detected by a CCD camera, which is also used to determine their position $x_0$ (*SI Text*, section 5). If initially more than one position in the cavity is occupied, blocking the trapping beam for short intervals allows loosing surplus particles for our measurements. To move the trapped particle to different positions along the cavity, we blue-detune the control laser to heat the CM degree of freedom of the particle. The "hot" particle moves across the standing wave until the control beam is switched off and the particle stays trapped at its new position (Fig. 2*B*).

**Readout of Control Beam.** For the position readout of the submicron particle motion, we rely on the dispersive interaction with the control field cavity mode. The control laser beam is initially prepared with a frequency difference of $\delta\omega \approx 2\pi \times 13.67$ GHz with respect to the original laser frequency $\omega_0$. When the control beam is transmitted through the cavity, it experiences a phase shift according to its detuning from the resonance $\omega_{cav}$. Because the particle position in the cavity modifies the cavity resonance frequency $\omega_{cav}$, a phase readout of the transmitted control beam allows reconstructing the submicron particle's motion. To detect the phase modulation introduced by the particle motion along the cavity, we spatially overlap the control beam (<0.1 mW) with an orthogonally polarized local oscillator (LO) (3.15 mW; at frequency $\omega_0$) at PBS4. A half-wave plate rotates the polarization of the beam by 45° resulting in interference of the control beam and the LO in the two output ports of PBS5 (Fig. 1). These optical signals are then detected at photodetectors PD1 and PD2 (Discovery Semiconductor; DSC-R410), which are fast enough to process the beat signal at frequency $\delta\omega$. To detect the full optical signal, we take the difference $I(t)$ of both detector outputs. This eliminates the DC part in the detection. The heterodyne measurement outcome $I(t)$ contains the beat signal with an offset phase $\phi_{\mathrm{opt}}$, which is determined by the unknown path difference between the LO and the control beam. The beat signal carries side bands representing the amplitude and phase modulation imprinted on the control beam by the optomechanical system. We demodulate $I(t)$ with an electronic local oscillator (ELO) with frequency $\delta\omega$ and phase $\phi_{\mathrm{ELO}}$ (relative to the beat signal). From the resulting signal $s_{\mathrm{opt}}(t)$, we extract the phase modulation of $I(t)$ by adjusting $\phi_{\mathrm{ELO}}$ such that the total phase $\phi_{\mathrm{ELO}} + \phi_{\mathrm{opt}} = \pi/2$. This is achieved by locking the DC part of $\langle s_{\mathrm{opt}}(t) \rangle$ to zero. We record the NPS of $s_{\mathrm{opt}}(t)$ with a spectrum analyzer, which allows reconstructing the NPS of the submicron particle's motion in postprocessing.

**Note Added in Proof.** Related work on cavity cooling of free nanoparticles has recently been reported by P. Asenbaum et al., in arXiv:1306.4617 (49).

**ACKNOWLEDGMENTS.** We thank O. Romero-Isart, A. C. Pflanzer, J. I. Cirac, P. Zoller, H. Ritsch, C. Genes, S. Hofer, G. D. Cole, W. Wieczorek, M. Arndt, and T. Wilk for stimulating discussions and support, and J. Schmöle for his graphical contributions. We acknowledge funding from the Austrian Science Fund (FWF) [Sonderforschungsbereich Foundations and Applications of Quantum Science (FOQUS)], the European Commission (Integrated Project Quantum Interfaces, Sensors and Communication based on Entanglement Q-ESSENCE, International Training Network Cavity Quantum Optomechanics cQOM), the European Research Council (ERC Starting Grant Quantum Optomechanics), The John Templeton Foundation (RQ-8251), and the European Space Agency (AO/1-6889/11/NL/CBi). N.K. acknowledges support by the Alexander von Humboldt Stiftung. U.D. and D.G. acknowledge support through the Doctoral Programme Complex Quantum Systems (CoQuS). R.K. acknowledges support from the Austrian Academy of Sciences through an APART Fellowship and from the European Commission through a Marie Curie Reintegration Grant. M.A. and R.K. acknowledge support through the Keck Institute for Space Studies.

1. Blatt R, Roos CF (2012) Quantum simulations with trapped ions. *Nat Phys* 8(4): 277–284.
2. Bloch I, Dalibard J, Nascimbène S (2012) Quantum simulations with ultracold quantum gases. *Nat Phys* 8(4):267–276.
3. Kielpinski D, Monroe C, Wineland DJ (2002) Architecture for a large-scale ion-trap quantum computer. *Nature* 417(6890):709–711.
4. Ritter S, et al. (2012) An elementary quantum network of single atoms in optical cavities. *Nature* 484(7393):195–200.
5. Hofmann J, et al. (2012) Heralded entanglement between widely separated atoms. *Science* 337(6090):72–75.
6. Hornberger K, Gerlich S, Haslinger P, Nimmrichter S, Arndt M (2012) Colloquium: Quantum interference of clusters and molecules. *Rev Mod Phys* 84(1):157–173.
7. Aspelmeyer M, Meystre P, Schwab K (2012) Quantum optomechanics. *Phys Today* 65(7):29–35.
8. Aspelmeyer M, Kippenberg T, Marquardt F (2013) Cavity optomechanics. arXiv: 1303.0733v1.
9. Chang DE, et al. (2010) Cavity opto-mechanics using an optically levitated nanosphere. *Proc Natl Acad Sci USA* 107(3):1005–1010.
10. Romero-Isart O, Juan ML, Quidant R, Cirac JI (2010) Toward quantum superposition of living organisms. *New J Phys* 12(3):033015.
11. Romero-Isart O, et al. (2011) Large quantum superpositions and interference of massive nano-objects. *Phys Rev Lett* 107(2):020405.
12. Geraci A, Papp S, Kitching J (2010) Short-range force detection using optically cooled levitated microspheres. *Phys Rev Lett* 105(10):101101.
13. Arvanitaki A, Geraci AA (2013) Detecting high-frequency gravitational waves with optically levitated sensors. *Phys Rev Lett* 110(7):071105.
14. Horak P, Hechenblaikner G, Gheri K, Stecher H, Ritsch H (1997) Cavity-induced atom cooling in the strong coupling regime. *Phys Rev Lett* 79(25):4974–4977.
15. Vuletić V, Chu S (2000) Laser cooling of atoms, ions, or molecules by coherent scattering. *Phys Rev Lett* 84(17):3787–3790.
16. Ashkin A, Dziedzic JM (1977) Feedback stabilization of optically levitated particles. *Appl Phys Lett* 30(4):202–204.
17. Li T, Kheifets S, Raizen MG (2011) Millikelvin cooling of an optically trapped microsphere in vacuum. *Nat Phys* 7(7):527–530.
18. Gieseler J, Deutsch B, Quidant R, Novotny L (2012) Subkelvin parametric feedback cooling of a laser-trapped nanoparticle. *Phys Rev Lett* 109(10):103603.
19. Koch M, et al. (2010) Feedback cooling of a single neutral atom. *Phys Rev Lett* 105(17): 173003.
20. Ye J, Vernooy DW, Kimble HJ (1999) Trapping of single atoms in cavity qed. *Phys Rev Lett* 83(24):4987–4990.
21. McKeever J, et al. (2003) State-insensitive cooling and trapping of single atoms in an optical cavity. *Phys Rev Lett* 90(13):133602.
22. Maunz P, et al. (2004) Cavity cooling of a single atom. *Nature* 428(6978):50–52.
23. Leibrandt DR, Labaziewicz J, Vuletic V, Chuang IL (2009) Cavity sideband cooling of a single trapped ion. *Phys Rev Lett* 103(10):103001.
24. Stute A, et al. (2012) Tunable ion-photon entanglement in an optical cavity. *Nature* 485(7399):482–485.
25. Hechenblaikner G, Gangl M, Horak P, Ritsch H (1998) Cooling an atom in a weakly driven high-q cavity. *Phys Rev A* 58(4):3030–3042.
26. Gangl M, Ritsch H (2000) 3d dissipative motion of atoms in a strongly coupled driven cavity. *Eur Phys J D* 8(1):29–40.
27. Favero I, et al. (2009) Fluctuating nanomechanical systems in a high finesse optical microcavity. *Opt Express* 17(15):12813–12820.
28. Anetsberger G, et al. (2009) Near-field cavity optomechanics with nanomechanical oscillators. *Nat Phys* 5(12):909–914.
29. Chan J, et al. (2011) Laser cooling of a nanomechanical oscillator into its quantum ground state. *Nature* 478(7367):89–92.
30. Thompson JD, et al. (2008) Strong dispersive coupling of a high finesse cavity to a micromechanical membrane. *Nature* 452(7183):72–76.
31. Teufel JD, et al. (2011) Sideband cooling of micromechanical motion to the quantum ground state. *Nature* 475(7356):359–363.
32. Purdy TP, Peterson RW, Regal CA (2013) Observation of radiation pressure shot noise on a macroscopic object. *Science* 339(6121):801–804.

33. Safavi-Naeini AH, et al. (2012) Observation of quantum motion of a nanomechanical resonator. *Phys Rev Lett* 108(3):033602.
34. Murch KW, Moore KL, Gupta S, Stamper-Kurn DM (2008) Observation of quantum-measurement backaction with an ultracold atomic gas. *Nat Phys* 4(7):561–564.
35. Purdy T, et al. (2010) Tunable cavity optomechanics with ultracold atoms. *Phys Rev Lett* 105(13):133602.
36. Schleier-Smith MH, Leroux ID, Zhang H, Van Camp MA, Vuletić V (2011) Optomechanical cavity cooling of an atomic ensemble. *Phys Rev Lett* 107(14):143005.
37. Kaltenbaek R, et al. (2012) Macroscopic quantum resonators (maqro). *Exp Astron* 34(2):123–164.
38. Ashkin A (2007) *Optical Trapping and Manipulation of Neutral Particles Using Lasers* (World Scientific Publishing, Singapore).
39. Nimmrichter S, Hammerer K, Asenbaum P, Ritsch H, Arndt M (2010) Master equation for the motion of a polarizable particle in a multimode cavity. *New J Phys* 12(8):083003.
40. Hammerer K, et al. (2009) Strong coupling of a mechanical oscillator and a single atom. *Phys Rev Lett* 103(14):063005.
41. Romero-Isart O, et al. (2011) Optically levitating dielectrics in the quantum regime: Theory and protocols. *Phys Rev A* 83(1):013803.
42. Barker PF, Shneider MN (2010) Cavity cooling of an optically trapped nanoparticle. *Phys Rev A* 81(2):023826.
43. Stamper-Kurn D (2012) Cavity optomechanics with cold atoms. arXiv:1204.4351v1.
44. Monteiro TS, et al. (2013) Dynamics of levitated nanospheres: Towards the strong coupling regime. *New J Phys* 15(1):015001.
45. Ashkin A, Dziedzic JM (1976) Optical levitation in high vacuum. *Appl Phys Lett* 28(6): 333–335.
46. Romero-Isart O (2011) Quantum superposition of massive objects and collapse models. *Phys Rev A* 84(5):052121.
47. Lechner W, Habraken SJM, Kiesel N, Aspelmeyer M, Zoller P (2013) Cavity optomechanics of levitated nanodumbbells: Nonequilibrium phases and self-assembly. *Phys Rev Lett* 110(14):143604.
48. Summers MD, Burnham DR, McGloin D (2008) Trapping solid aerosols with optical tweezers: A comparison between gas and liquid phase optical traps. *Opt Express* 16(11):7739–7747.
49. Asenbaum P, Kuhn S, Nimmrichter S, Sezer U, Arndt M (2013) Cavity cooling of free silicon nanoparticles in high-vacuum. arXiv:1306.4617.